ELSEVIER

Biochimica et Biophysica Acta 1461 (1999) 83–95

BIOCHIMICA ET BIOPHYSICA ACTA
BBA

www.elsevier.com/locate/bba

N-terminal chimeric constructs improve the expression of sarcoplasmic reticulum Ca^{2+}-ATPase in yeast

Eduardo M.R. Reis [a], Eleonora Kurtenbach [b], Alessandra R. Ferreira [a], Paolo J.C. Biselli [a], Carolyn W. Slayman [c], Sergio Verjovski-Almeida [a,*]

[a] *Departamento de Bioquímica, Instituto de Química, Universidade de São Paulo, 05508-900 São Paulo, S.P., Brazil*
[b] *Departamento de Bioquímica Médica, Instituto de Ciências Biomédicas, Universidade Federal do Rio de Janeiro, 21944-590 Rio de Janeiro, R.J., Brazil*
[c] *Department of Human Genetics, Yale University School of Medicine, New Haven, CT 06510, USA*

Received 19 May 1999; received in revised form 31 August 1999; accepted 31 August 1999

Abstract

Wild-type and chimeric constructs comprising rabbit sarcoplasmic reticulum (SR) Ca^{2+}-ATPase and the N-terminal cytoplasmic portion of yeast plasma membrane H^+-ATPase were expressed in yeast under control of a heat-shock regulated promoter. The wild-type ATPase was found predominantly in endoplasmic reticulum (ER) membranes. Addition of the first 88 residues of H^+-ATPase to the Ca^{2+}-ATPase N-terminal end promoted a marked shift in the localization of chimeric H^+/Ca^{2+}-ATPase which accumulated in a light membrane fraction associated with yeast smooth ER. Furthermore, there was a three-fold increase in the overall level of expression of chimeric H^+/Ca^{2+}-ATPase. Similar results were obtained for a chimeric Ca^{2+}-ATPase containing a hexahistidine sequence added to its N-terminal end. Both H^+/Ca^{2+}-ATPase and $6\times$His-Ca^{2+}-ATPase were functional as demonstrated by their ability to form a phosphorylated intermediate and undergo fast turnover. Conversely, a replacement chimera in which the N-terminal end of SR Ca^{2+}-ATPase was replaced by the corresponding segment of H^+-ATPase was not stably expressed in yeast membranes. These results indicate that the N-terminal segment of Ca^{2+}-ATPase plays an important role in enzyme assembly and contains structural determinants necessary for ER retention of the ATPase.

Keywords: Ca^{2+}-ATPase; Endoplasmic reticulum; Heterologous expression; Membrane targeting; *Saccharomyces cerevisiae*

1. Introduction

Sarcoplasmic reticulum (SR) Ca^{2+}-ATPase is an integral membrane enzyme that transports calcium from the cytoplasm into the reticulum lumen of muscle cells and plays a critical role in the physiology of muscle relaxation. Over the past 10 years, studies on site-specific mutants produced in mammalian cells have led to significant progress in defining structure-function relationships throughout the ATPase polypeptide [1,2]. However, the low level of SR Ca^{2+}-ATPase expressed in COS-1 cells has prevented the direct measurement of hydrolytic activity and ligand-binding constants [3,4]. Larger quantities of SR Ca^{2+}-ATPase can be produced in the baculovirus expression system [5]. Notwithstanding, the excessive amount of transfected insect cells required for ligand-

* Corresponding author. Fax: +55-11-818-2186; E-mail: verjo@iq.usp.br, http://www.iq.usp.br/wwwchem/bioquimica/

0005-2736/99/$ – see front matter
PII: S0005-2736(99)00151-0

binding studies renders this expression system unsuitable for analyzing large numbers of mutants.

In parallel with these efforts, several laboratories have worked to express SR Ca^{2+}-ATPase in yeast, which offers a powerful array of genetic and cell biological methods to dissect protein function. While it is clear that functional SR Ca^{2+}-ATPase can be obtained in yeast, quantities are limited and do not yet permit biochemical and biophysical studies [6–8]. Furthermore, the subcellular localization of yeast-expressed SR Ca^{2+}-ATPase has been controversial in the literature. Centeno et al. [6] have shown that SR Ca^{2+}-ATPase expressed in yeast under control of the *GAL10* promoter accumulates in several internal membranes. In their work, the Ca^{2+}-ATPase was predominantly recovered in a fraction that was believed to contain plasma membranes [6], though it failed to co-localize with the yeast plasma membrane H^+-ATPase upon sucrose gradient fractionation. When secretory vesicles were isolated from a *sec*-deficient strain expressing SR Ca^{2+}-ATPase, Ca^{2+}-dependent ATPase activity could be measured with a coupled enzyme assay. Thus, it was proposed that a significant amount of the recombinant Ca^{2+}-ATPase was trapped in secretory vesicles en route to the yeast plasma membrane [6]. In contrast, Degand et al. [7] recently showed by sucrose gradient fractionation and immunogold electron microscopy that the SR Ca^{2+}-ATPase, in this case expressed under control of the constitutive *PMA1* promoter, was mainly localized to yeast membranes derived from the endoplasmic reticulum (ER). The recombinant Ca^{2+}-ATPase was functional in vivo, as demonstrated by its ability to restore growth of mutant host cells deprived of the endogenous organellar Ca^{2+}-ATPase PMR1 and PMC1 [7].

In a previous study, we have shown the expression of SR Ca^{2+}-ATPase in yeast under control of a heat shock-activated promoter [8]. The heat shock-induced SR Ca^{2+}-ATPase appeared by immunofluorescence microscopy to be localized in yeast internal membranes and was functional, since a detergent-solubilized and immunoprecipitated preparation was able to form a phosphorylated intermediate in the presence of Ca^{2+} and ATP [9]. In the work to be described below, we have aimed to improve expression by constructing N-terminal chimeras between SR Ca^{2+}-ATPase and yeast plasma membrane H^+-ATPase and testing the ability of signal sequences from the latter to direct the H^+/Ca^{2+}-ATPase chimera to the plasma membrane. This approach was motivated by the fact that the N-terminal sequence from yeast H^+-ATPase was previously shown to be necessary to target this enzyme to the plasma membrane [10]. Two types of chimeric constructs were devised: in one of them, the N-terminal cytoplasmic moiety of yeast plasma membrane H^+-ATPase was added to SR Ca^{2+}-ATPase immediately before the initial methionine (additive chimeric H^+/Ca^{2+}-ATPase). In a second construct, the N-terminal H^+-ATPase sequence was substituted for the N-terminal moiety of SR Ca^{2+}-ATPase (replacement chimeric $H^+\Delta Ca^{2+}$-ATPase). A third construct, a SR Ca^{2+}-ATPase chimera containing a hexahistidine motif added to its N-terminal methionine, was tested in parallel to observe the effect of addition of an unrelated sequence on the stability and activity of the Ca^{2+}-ATPase. Although the replacement chimera was not expressed in yeast, both the additive chimera and the hexahistidine chimera were produced at three-fold higher levels than unmodified SR Ca^{2+}-ATPase. In both cases, most of the chimeric protein accumulated in a distinct light ER subcompartment, as opposed to wild-type Ca^{2+}-ATPase, which accumulated in heavy ER. Thus, the exogenous sequences introduced in the N-terminal region did modify ER retention determinants but were not sufficient to direct the Ca^{2+}-ATPase chimeras to the plasma membrane.

2. Materials and methods

2.1. Strains and media

Saccharomyces cerevisiae strain NY605 (*MAT*a; *ura*3-12; *leu*2-3,112; *GAL*), provided by Dr. Peter Novick (Department of Cell Biology, Yale University School of Medicine), was used as the host organism for the expression of rabbit SR Ca^{2+}-ATPase. Secretory-deficient strain SY2 (*MAT*a; *ura*3-52; *leu*2-3,112; *his*4-619; *sec*6-4; *GAL*) was used for characterization of Ca^{2+}-ATPase expression in secretory vesicles. Yeast cells were transformed by the method of Elble [11]. Transformed NY605 cells were selected and propagated on minimal medium

containing 2% glucose and supplemented with 20 mg uracil/l. Transformed SY2 cells were selected in the same medium additionally supplemented with 20 mg histidine/l.

2.2. Plasmid constructions

The cloned 2991 bp cDNA from fast-twitch rabbit SR Ca^{2+}-ATPase [12] was kindly provided by Dr. David MacLennan (University of Toronto). Unique restriction sites *Hin*dIII and *Sac*I were introduced by PCR in the 5′ and 3′ non-coding flanking regions of the Ca^{2+}-ATPase gene, respectively, by standard techniques [13]. The upstream primer used for introducing the *Hin*dIII site was 5′ CC AAG CTT AAA TTA ATA ATG GAG GCC GCG CAC TC 3′ (non-homologous sequence is underlined), which simultaneously introduced an A at position −3 for proper translation initiation in yeast [14]. The *Hin*dIII-*Sac*I fragment containing the Ca^{2+}-ATPase cDNA was then moved to the yeast episomal plasmid YEplac181 [15]. To optimize expression, a *Sal*I-*Hin*dIII fragment containing two in tandem copies of the yeast heat shock element (*HSE2*) [16] was cloned immediately before the 5′ end of the Ca^{2+}-ATPase cDNA, and a 650 bp fragment containing the transcription termination consensus sequence from the 3′ non-coding region of the yeast *PMA1* gene [17] was cloned immediately after the 3′ end of the Ca^{2+}-ATPase cDNA. The final construct has been designated pSVA12.

Plasmid pARF1 was derived from pSVA12 and from pPROEX-1 (Life Technologies, Gaithersburg, MD) to generate a hexahistidine-tagged Ca^{2+}-ATPase cDNA. Two rounds of PCR were performed using these plasmids as templates in order to create appropriate restriction sites for cloning. Firstly, a 187 bp fragment obtained by PCR amplification of vector pPROEX-1 with primers 5′ ACC AAG CTT AAA TTA ATA ATG GGT CAT CAT CAT CAT CAT C 3′ (forward) and 5′ C AAG CTT GGC TGT TTT GGC G 3′ (reverse) was digested with *Hin*dIII and cloned on a *Hin*dIII-digested pBlueScript II (Stratagene, LaJolla, CA) giving vector pHexaHis. Secondly, a *Nde*I restriction site was introduced on the 5′ end of the Ca^{2+}-ATPase coding sequence by PCR amplification of plasmid pSVA12 with primers 5′ ATC AAG CTT AAA TTA CAT ATG GAG GCC G 3′ (forward) and 5′ CAG CTG CTC CCC GAA CTC ATC C 3′ (reverse). The 790 bp amplified fragment was digested with *Nde*I and *Kpn*I and cloned on *Nde*I-*Kpn*I-digested pHexaHis giving vector pHexaHis-N-ATP. Dideoxy sequencing confirmed the correct frame for the ATG translation initiation codon followed by the sequence coding for six histidines plus a seven amino acid spacer region and a seven amino acid site for rTEV protease cleavage (from the pPROEX-1 vector, Life Technologies, Gaithersburg, MD) which were joined to the amino-terminal residues from SR Ca^{2+}-ATPase. pHexaHis-N-ATP was digested with *Hin*dIII and *Stu*I and the 140 bp *Hin*dIII-*Stu*I fragment was cloned into *Hin*dIII-*Stu*I-digested pSVA12.

Two chimeric plasma membrane H^+-ATPase/SR Ca^{2+}-ATPase constructs were obtained. In one of them, a replacement chimeric $H^+\Delta Ca^{2+}$-ATPase, residues Met1–Leu24 from Ca^{2+}-ATPase were replaced by the first 88 residues from yeast plasma membrane H^+-ATPase. To that end, the yeast *PMA1* gene [18] was used as a template for PCR amplification with primers 5′ GAA CGG AAT TCA GAA AAT CAT TGA AAA GAA TAA GAA G 3′ (forward) and 5′ CAT CGG AAT TCA GGC CTG TAG ATG GGT CAG TTT GTA AAT ATT C 3′ (reverse). The 344 bp amplified fragment contained the sequence coding for the 88 amino acid residues of H^+-ATPase flanked by an *Eco*RI restriction site at its 5′ non-coding end and *Stu*I-*Eco*RI restriction sites at its 3′ end. This fragment was digested with *Eco*RI, cloned into *Eco*RI-digested pBlueScript II and fully sequenced by the dideoxy method. This construct was designated pN-PMA1. pN-PMA1 was digested with *Hin*dIII-*Stu*I and the 292 bp *Hin*dIII-*Stu*I fragment was ligated to *Hin*dIII-*Stu*I-treated pSVA12 giving plasmid pSVA21. A second, additive H^+/Ca^{2+}-ATPase chimera was constructed by placing the first 88 residues from yeast plasma membrane H^+-ATPase immediately before Met1 of Ca^{2+}-ATPase. To that end, plasmid pARF1 was digested with *Nde*I, made blunt with Klenow and digested with *Hin*dIII to remove the fragment containing the hexahistidine sequence. pN-PMA1 was digested with *Hin*dIII-*Stu*I and the 292 bp *Hin*dIII-*Stu*I fragment was ligated to *Nde*I-Klenow-*Hin*dIII-treated pARF1 giving pVVL1.

2.3. Induction of SR Ca^{2+}-ATPase synthesis and isolation of membranes

Transformed yeast cells (strain NY605) were grown at 23°C in glucose minimal medium supplemented with uracil to early-log phase ($OD_{600} \sim 0.5$) and then shifted to 37°C for 90 min. Preparation of cell lysates was essentially as described by Perlin et al. [19]. Following a low speed ($418 \times g$ for 3 min) centrifugation for removal of unbroken cells and large debris, the lysate was sequentially spun at medium speed (two times $24\,000 \times g$ for 20 min) and high speed ($135\,000 \times g$ for 1 h). The resulting pellets were resuspended in the original volume of homogenization buffer by use of a Potter-Elvehjem tissue grinder and stored at −80°C. Alternatively, the $24\,000 \times g$ pellet was resuspended at 1400 OD_{600}/ml in 50 mM MOPS, pH 7.5, 0.3 M sucrose, 1 mM $CaCl_2$ in order to concentrate the Ca^{2+}-ATPase for functional assays. Protease inhibitors were included in the homogenization buffer and in all subsequent steps at the following concentrations: diisopropyl fluorophosphate, 1 mM; chymostatin, 5 μg/ml; and leupeptin, pepstatin and aprotinin, 2 μg/ml each.

2.4. Sucrose gradient fractionation

Yeast lysates were fractionated by sucrose gradient centrifugation essentially as described by Antebi and Fink [20].

2.5. Isolation of secretory vesicles

Secretory vesicles were isolated as described by Ambesi et al. [21], using *sec*-deficient cells expressing either wild-type Ca^{2+}-ATPase or N-tagged Ca^{2+}-ATPase.

2.6. Protein methods and enzyme assays

Protein concentration was determined by the method of Lowry et al. [22] using bovine serum albumin as a standard. Guanosine diphosphatase was assayed according to Abeijon et al. [23]. NADPH-cytochrome *c* reductase was assayed as described by Feldman et al. [24]. Vanadate-sensitive H^+-ATPase activity was measured ad described by Nakamoto et al. [16].

2.7. Electrophoretic and immunological methods

For Western blots, electrotransfer of proteins from SDS gels to nitrocellulose membranes and blocking with non-fat milk were performed according to standard procedures [25]. Monoclonal antibody against rabbit SR Ca^{2+}-ATPase (A52) was diluted 1:2000 and detected with the ECL-luminol kit (Amersham-Pharmacia). For quantitative dot-blots one of the following antibodies was used: monoclonal antibody A52 (1:2000 dilution), yeast endoplasmic reticulum BiP/Kar2 antiserum [26] (1:5000 dilution) or a polyclonal antibody against *Neurospora crassa* plasma membrane H^+-ATPase [27] (1:2000 dilution). Following incubation with 2 μCi protein A-^{125}I for 2 h, the bound antibodies were detected by exposure to an autoradiography film (Hyperfilm/Amersham-Pharmacia). The relative amounts of Ca^{2+}-ATPase, BiP/Kar2 or H^+-ATPase present in each fraction, expressed in integrated optical density units (IOD), were determined using the ImageMaster VDS densitometer and software (Amersham-Pharmacia). Quantitation of expressed Ca^{2+}-ATPase was estimated by comparison with SR Ca^{2+}-ATPase purified from rabbit muscle and spotted on the dot-blot membranes.

2.8. Immunofluorescence microscopy

Fixation and immunofluorescent staining of induced yeast cells were performed essentially as described by Pringle et al. [28]. The slides were incubated overnight with a mouse monoclonal antibody against rabbit SR Ca^{2+}-ATPase (mAb Cl-30) diluted 1:30 plus rabbit polyclonal antibody against yeast endoplasmic reticulum BiP/Kar2 diluted 1:1000. After 2 h incubation with secondary antibodies (Sigma, USA) against mouse IgG labelled with tetramethyl-rhodamine isothiocyanate and rabbit IgG labelled with fluorescein isothiocyanate (diluted 1:300), the slides were mounted with *p*-phenylenediamine. Fluorescence and differential interference contrast images were acquired using a Zeiss PlanApochro-

matic 100×1.4 NA objective on a Zeiss Axiovert 100 microscope attached to a Bio-Rad MRC-1024 UV confocal laser scanning system.

2.9. Immunoprecipitation of SR Ca^{2+}-ATPase

The 24 000×*g* yeast membrane fraction described in Section 2.3 was used for detergent solubilization and immunoprecipitation of heterologous Ca^{2+}-ATPase as described by Skerjanc et al. [5] using 3 mg of a monoclonal antibody raised against rabbit SR Ca^{2+}-ATPase (mAb Cl-30) and 30 μl protein A-Sepharose (Amersham-Pharmacia).

2.10. Phosphoenzyme formation and turnover

Phosphoenzyme formation was carried out by incubation of the immunoprecipitated Ca^{2+}-ATPase in 30 μl of phosphorylation buffer (50 mM MOPS, pH 6.5, 80 mM KCl, 10 mM $MgCl_2$, 0.1 mM $CaCl_2$, 1 mg/ml $C_{12}E_8$, 0.5 mg/ml asolectin) containing 10 μM [γ-^{32}P]ATP and 100 μM $CaCl_2$ for 10 s at 4°C, as described by Clarke et al. [4]. The phosphorylation reaction was stopped by addition of 0.5 ml ice-cold 10% trichloroacetic acid (TCA) and acid-washed by centrifugation as described [4]. When indicated in Section 3, addition of 100 μl of phosphorylation buffer containing 250 μM cold ATP before stopping the reaction with acid was performed to determine the decay rate of phosphoenzyme intermediate. Following separation by acidic SDS-PAGE [4] the E-^{32}P intermediate was detected by autoradiography.

3. Results

3.1. Effect of N-terminal sequence tags on SR Ca^{2+}-ATPase expression

The first goal of this study was to ask whether modification of the N-terminus would affect the expression of SR Ca^{2+}-ATPase in yeast. To that end, an 88 amino acid sequence from yeast *PMA1* [18] stretching from the initial methionine to the N-terminal conserved consensus Gly-Leu of P-type ATPases was either substituted for the 24 amino residues of SR Ca^{2+}-ATPase ($H^+\Delta Ca^{2+}$-ATPase) or fused to the initial methionine of SR Ca^{2+}-ATPase (H^+/Ca^{2+}-ATPase). To test the effect of an unrelated sequence upon Ca^{2+}-ATPase expression, a 24 amino acid sequence containing a hexahistidine motif (plus a spacer region and a protease cleavage site) was added to the N-terminus of the SR Ca^{2+}-ATPase (6×His-Ca^{2+}-ATPase). The cDNAs encoding $H^+\Delta Ca^{2+}$-ATPase, H^+/Ca^{2+} ATPase and 6×His-Ca^{2+}-ATPase fusion proteins were cloned into pSVA12 to give plasmids pSVA21, pVVL1 and pARF1, respectively. NY605 cells were transformed with these plasmids, grown at 23°C, and shifted to 37°C for induction. After 2 h of incubation at 37°C, total lysates were analyzed by Western blotting with an anti-Ca^{2+}-ATPase monoclonal antibody and a peroxidase-conjugated secondary antibody.

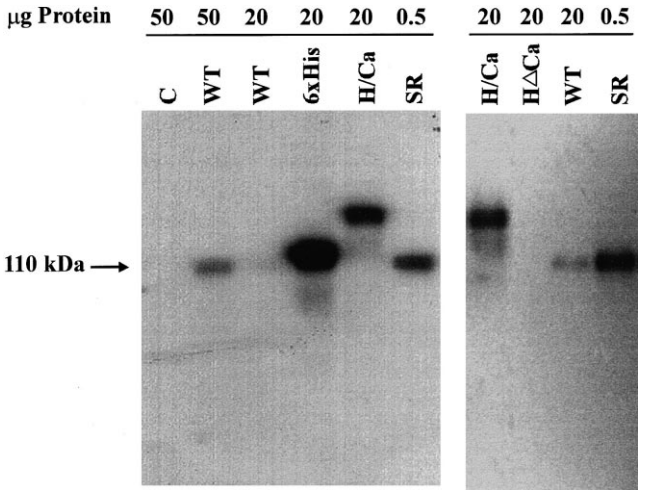

Fig. 1. Expression of N-terminal-tagged Ca^{2+}-ATPase. Total lysates from induced cells expressing wild-type SR Ca^{2+}-ATPase (WT), hexahistidine-tagged Ca^{2+}-ATPase (6×His), additive chimeric H^+/Ca^{2+} ATPase (H/Ca) or replacement H^+/Ca^{2+} ATPase (HΔCa) were analyzed by Western blotting. Lysate from yeast transformed with an empty plasmid served as a negative control (C), and 0.5 μg of Ca^{2+}-ATPase purified from rabbit muscle sarcoplasmic reticulum served as a positive control (SR). Samples of 20 μg or 50 μg of total yeast protein were separated by 10% SDS-PAGE and transferred to a nitrocellulose membrane. Recombinant Ca^{2+}-ATPase was detected by immunoblot using a monoclonal antibody specific for fast-twitch Ca^{2+}-ATPase and a peroxidase-conjugated secondary antibody.

Both H^+/Ca^{2+}-ATPase and 6×His-Ca^{2+}-ATPase were expressed with the expected size and displayed no significant degradation (Fig. 1, lanes H/Ca and 6×His). Conversely, there was no detectable expression of the $H^+\Delta Ca^{2+}$-ATPase chimera (Fig. 1,

HΔCa). No Ca^{2+}-ATPase could be detected in the empty plasmid control (Fig. 1, lane C), confirming that the monoclonal antibody was specific for recombinant Ca^{2+}-ATPases and did not cross-react with endogenous yeast ATPases. Inspection of the intensity of the bands when equal amounts of total protein were applied in the gel suggested that the Ca^{2+}-ATPase chimeras were expressed at a much higher level than wild-type Ca^{2+}-ATPase produced in the same conditions (Fig. 1, lanes WT, H/Ca and 6×His). Indeed, quantitative dot-blots described in detail in Section 3.2 showed a three-fold higher level of expression of the chimeras when compared with wild-type Ca^{2+}-ATPase, making clear that the electrotransfer used in the Western blot was not quantitative.

3.2. Recovery of wild-type and chimeric Ca^{2+}-ATPase in yeast membrane fractions

The amount of wild-type SR Ca^{2+}-ATPase per liter of induced yeast culture, as determined by quantitative dot-blotting, averaged 348 ± 58 μg, corresponding to approximately 0.3% of the protein present in the total yeast lysate (Table 1, panel A). Proper membrane insertion of SR Ca^{2+}-ATPase constructs was evaluated by the measurement of Ca^{2+}-ATPase recovery within yeast membrane fractions sedimenting with medium-speed (24 000×*g*) or high-speed (135 000×*g*) velocities. After removal of large cellular debris by low-speed centrifugation (418×*g*), 89% of the remaining SR Ca^{2+}-ATPase was recovered in the 24 000×*g* pellet, where it amounted to 2% of the protein present in that fraction. Further centrifugation at 135 000×*g* recovered an additional 7% of Ca^{2+}-ATPase (Table 1, panel A).

Quantitative dot-blotting of H^+/Ca^{2+}-ATPase and 6×His-Ca^{2+}-ATPase revealed that both chimeras were expressed at an elevated level of 850 μg/l of yeast culture (Table 1, panels B and C), corresponding to 1% of the protein present in total yeast lysate. When 418×*g* supernatants were fractionated, 61 and 53% of the remaining Ca^{2+}-ATPase was recovered in the 24 000×*g* pellet for H^+/Ca^{2+}-ATPase and 6×His-Ca^{2+}-ATPase, respectively (Table 1, panels B and C). The N-tagged Ca^{2+}-ATPase chimeras amounted to 6–7% of the total protein present in the 24 000×*g* membrane pellet (Table 1, panels B and C). Further centrifugation of the 24 000×*g* supernatant at 135 000×*g* recovered an additional 13 and 18% of the chimeric Ca^{2+}-ATPases (Table 1, panels B and C).

Thus, the majority of both wild-type and N-terminal-tagged Ca^{2+}-ATPase was recovered in the 24 000×*g* pellet fraction. The addition of either

Table 1
Recovery of heterologous rabbit Ca^{2+}-ATPase on yeast membrane fractions

Fraction	Yield[a] (μg/l)	Ca^{2+}-ATPase recovery	mg of Ca^{2+}-ATPase per mg of total protein
A: wt Ca^{2+}-ATPase			
Total lysate	348 ± 58 (4)	–	0.003
S 418×*g*	308 ± 34 (4)	1	0.003
P 24 000×*g*	275 ± 55 (4)	0.89	0.02
P 135 000×*g*	21 ± 11 (4)	0.07	0.01
B: H^+/Ca^{2+}-ATPase			
Total lysate	854 ± 51 (2)	–	0.01
S 418×*g*	756 ± 68 (2)	1	0.01
P 24 000×*g*	401 ± 55 (2)	0.61	0.07
P 135 000×*g*	137 ± 17 (2)	0.13	0.03
C: 6×His-Ca^{2+}-ATPase			
Total lysate	840 ± 76 (3)	–	0.01
S 418×*g*	729 ± 95 (3)	1	0.01
P 24 000×*g*	445 ± 53 (3)	0.53	0.06
P 135 000×*g*	92 ± 8 (3)	0.18	0.03

[a]Yield refers to μg of recombinant Ca^{2+}-ATPase produced per liter of induced yeast cell culture which corresponded to approximately 700 OD_{600} units. Ca^{2+}-ATPase content in each fraction was determined by quantitative dot-blot using a monoclonal antibody against rabbit Ca^{2+}-ATPase and ^{125}I-protein A.

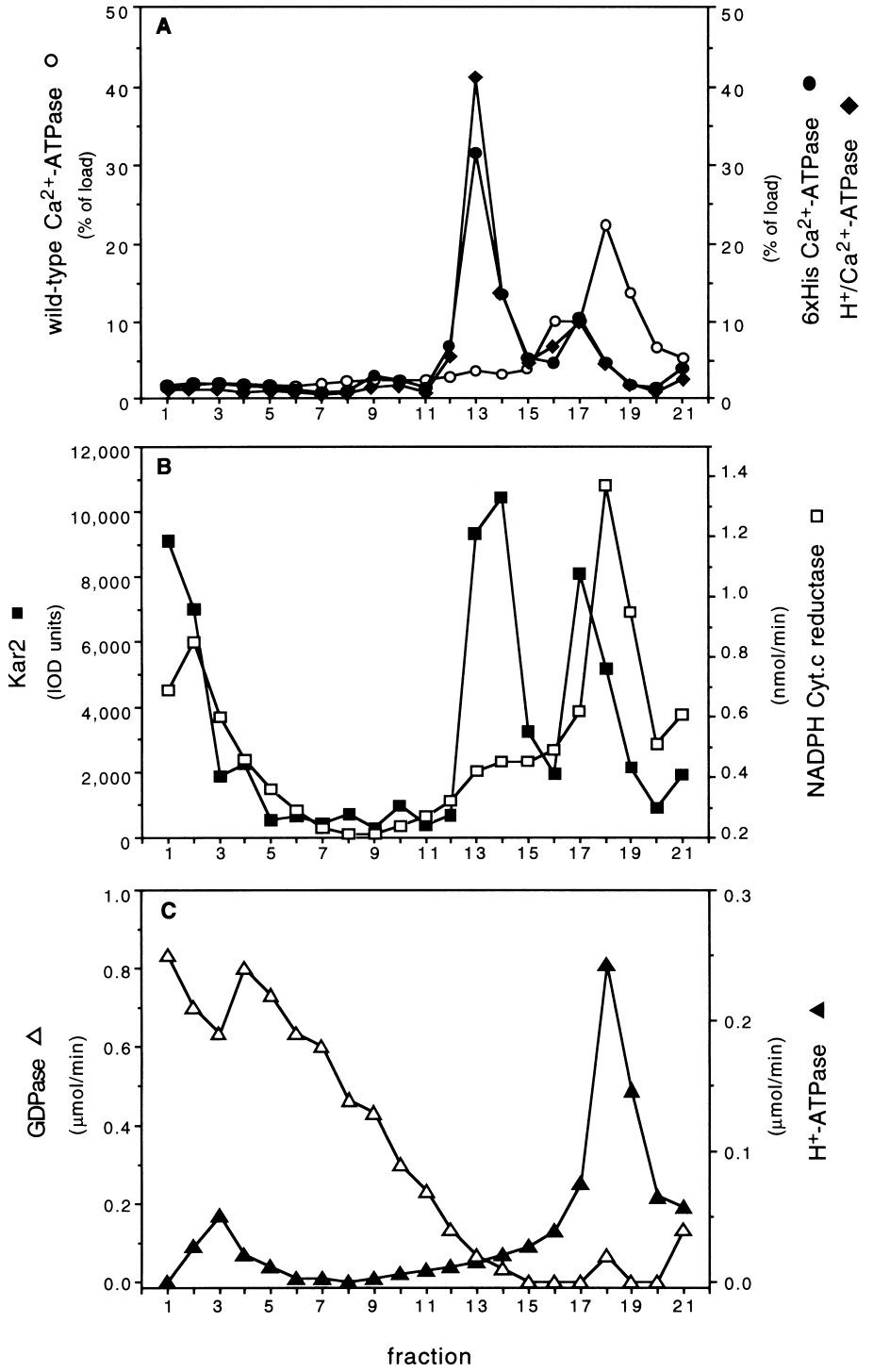

Fig. 2. Distribution of rabbit Ca^{2+}-ATPase and marker enzymes on a sucrose gradient. Yeast lysates prepared from induced cells transformed with plasmids containing the cDNA for wild-type SR Ca^{2+}-ATPase or N-tagged-Ca^{2+}-ATPase were fractionated by centrifugation on a discontinuous sucrose density gradient (15–60%). Gradient fractions of 1.5 ml were collected from top (fraction 1) to bottom (fraction 21) and assayed as described in Section 2. (A) Wild-type Ca^{2+}-ATPase (○), H^+/Ca^{2+}-ATPase (◆), 6×His-Ca^{2+}-ATPase (●). (B) BiP/Kar2 (■) and NADPH-cytochrome *c* reductase (□) (endoplasmic reticulum markers). (C) GDPase (△) (Golgi marker) and H^+-ATPase (▲) (plasma membrane marker).

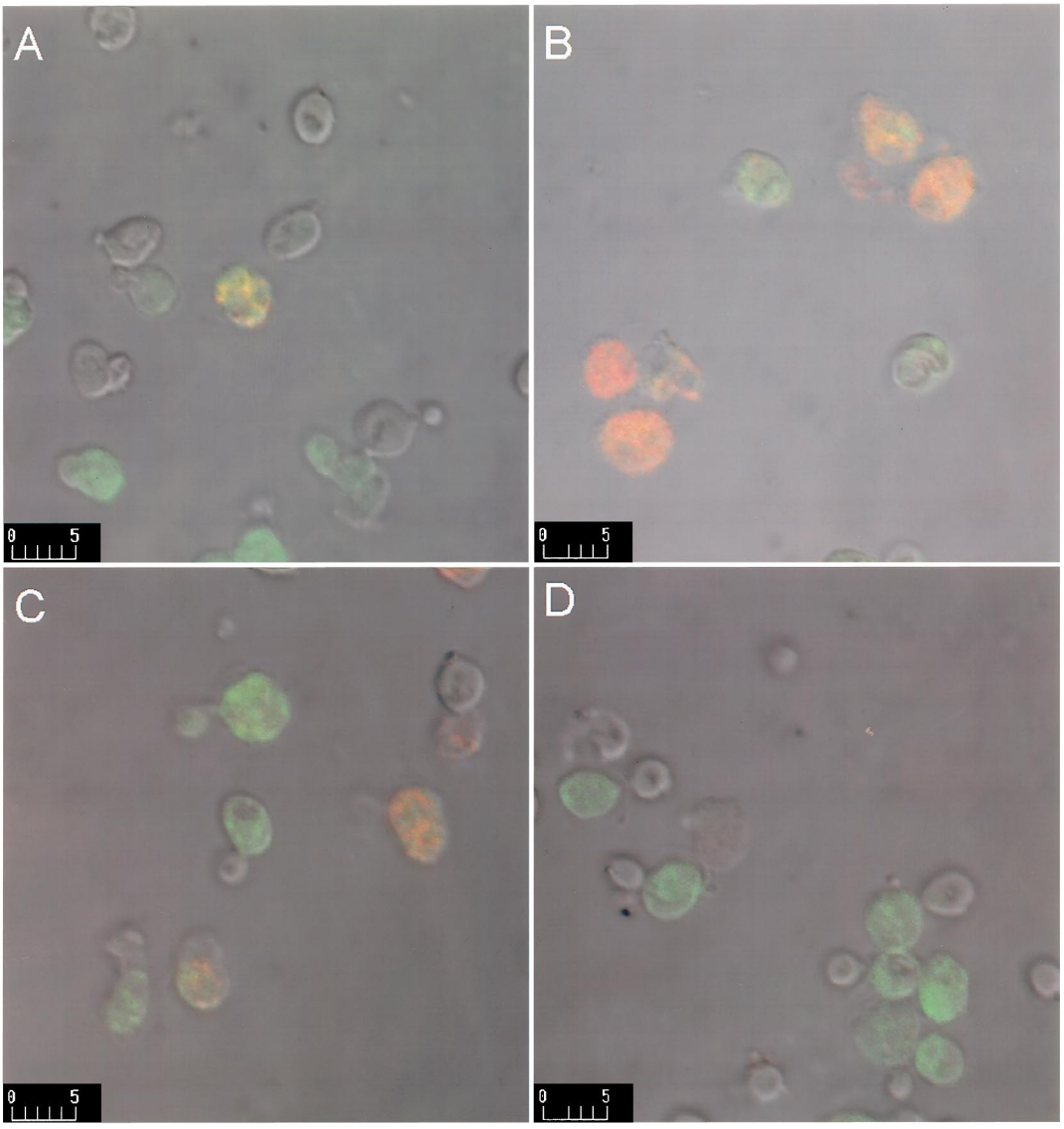

Fig. 3. Double-immunofluorescence localization of rabbit SR Ca^{2+}-ATPase expressed in yeast. Yeast cells expressing wild-type Ca^{2+}-ATPase (A), H^+/Ca^{2+} chimeric ATPase (B) or hexahistidine-tagged Ca^{2+}-ATPase (C) were fixed in 4% formaldehyde, converted to spheroplasts and immobilized on glass slides. The slides were incubated with mouse monoclonal antibody Cl-30 against SR Ca^{2+}-ATPase (dilution 1:30) plus rabbit polyclonal antibody against yeast BiP/Kar2 endoplasmic reticulum marker (dilution 1:1000) followed by rhodamine-conjugated anti-mouse secondary antibody (dilution 1:300) plus fluorescein-conjugated anti-rabbit secondary antibody (dilution 1:300). Yeast cells transformed with an empty plasmid were treated likewise and used as a negative control (D). Image acquisition was performed on an MRC-1024 Bio-Rad confocal laser microscope. Rhodamine fluorescence is shown in red, fluorescein is shown in green and they are superimposed on differential interference contrast gray images to highlight the cell contours. Calibration bars are in μm.

H^+-ATPase or hexahistidine N-terminal sequences caused a 2–3-fold increase in the amount of Ca^{2+}-ATPase present in total yeast lysates and a three-fold increase in the enrichment of SR Ca^{2+}-ATPase in the $24\,000\times g$ pellet fraction (going from 2% to 7% of total protein, see Table 1).

3.3. *Localization of wild-type and chimeric SR Ca^{2+}-ATPase on yeast internal membranes*

To determine the subcellular location of wild-type and chimeric SR Ca^{2+}-ATPase, transformed yeast cells were subjected to heat shock for 90 min, and

total lysates were fractionated by equilibrium centrifugation through a 15–60% discontinuous sucrose gradient. In Fig. 2, the fractionation profiles of wild-type and N-tagged Ca^{2+}-ATPase (panel A) were compared to the profiles of several yeast subcellular markers (panels B and C). Wild-type Ca^{2+}-ATPase co-sedimented with the ER marker NADPH-cytochrome *c* reductase, both displaying peaks in fraction 18 of the gradient (Fig. 2A,B). As expected, the wild-type Ca^{2+}-ATPase peak displayed a significant overlap with another ER marker, BiP/Kar2, that exhibited its typical bimodal distribution [29], with peaks in fractions 13 and 17 (Fig. 2B). The ATPase was well separated from GDPase activity, which served as a Golgi marker (Fig. 2C), but co-sedimented with vanadate-sensitive H^+-ATPase activity, a plasma membrane marker (Fig. 2C).

Curiously, both H^+/Ca^{2+}-ATPase- and 6×His-Ca^{2+}-ATPase-containing fractions exhibited a significant shift towards lighter regions of the gradient, as compared with wild-type Ca^{2+}-ATPase. Both chimeras displayed a predominant peak in fraction 13 (Fig. 2A), which co-sedimented with a light fraction of the ER marker BiP/Kar2 (Fig. 2B). A small, secondary peak containing chimeric Ca^{2+}-ATPase was recovered together with a heavy fraction of ER marker BiP/Kar2 in fraction 17 (Fig. 2A,B).

Next, immunofluorescence confocal laser microscopy was carried out to see whether the wild-type SR Ca^{2+}-ATPase was predominantly localized in the ER compartment or on the plasma membrane. Induced spheroplasts were double-labeled with a mouse anti-Ca^{2+}-ATPase monoclonal antibody and a rabbit polyclonal antiserum raised against ER marker BiP/Kar2. Following incubation with both rhodamine-conjugated anti-mouse IgG and fluorescein-conjugated anti-rabbit IgG, a significant yellow fluorescence signal resulting from the overlay of red (rhodamine-labeled Ca^{2+}-ATPase) and green (fluorescein-labeled BiP/Kar2) fluorescence could be detected in internal organelles, with little if any labeling at the cell periphery (Fig. 3A). This observation suggests the co-localization of wild-type Ca^{2+}-ATPase with BiP/Kar2 and is consistent with the idea that the recombinant enzyme is located in the ER. Subcellular localization of SR Ca^{2+}-ATPase chimeras was also evaluated by immunofluorescence confocal laser microscopy. A stronger yellow to orange immunofluorescence signal was observed in cells expressing either H^+/Ca^{2+}-ATPase or 6×His-Ca^{2+}-ATPase when compared with cells expressing wild-type Ca^{2+}-ATPase (Fig. 3A–C), correlating with the higher expression level seen by quantitative immunoblotting. The distribution of ATPase was somewhat heterogeneous and spread over much of the cytoplasm (Fig. 3A–C).

Expression in a secretory-deficient yeast strain (SY2) was devised as a conclusive test to see whether any SR Ca^{2+}-ATPase was able to move out of the ER. Upon shifting to 37°C, these cells accumulate secretory vesicles, which can be isolated and assayed for proteins en route to the plasma membrane [30]. In the experiment of Table 2, SY2 cells were transformed with plasmids pSVA12, pVVL1 or pARF1

Table 2
Recovery[a] of wild-type and chimeric SR Ca^{2+}-ATPase in yeast secretory vesicles

Fraction	Ca^{2+}-ATPase						Plasma membrane H^+-ATPase (%)	Endoplasmic reticulum Kar2 (%)
	wt		H^+/Ca^{2+}		6×His			
	IOD[b]	%	IOD	%	IOD	%		
Total lysate	8 656	–	15 200	–	45 016	–	–	–
Clarified lysate	528	100	760	100	1 576	100	100	100
High-speed pellet	156	30	699	84	1 271	81	75	20
Secretory vesicles	43	9	167	20	277	18	56	8

Clarified lysate is the supernatant of a 14 500×*g* centrifugation of the total lysate and High-speed pellet is obtained by a 100 000×*g* centrifugation of the clarified lysate as described in Section 2. Secretory vesicles were prepared from the high-speed pellet by sucrose gradient fractionation according to Ambesi et al. [21].

[a]Recovery of Ca^{2+}-ATPase, H^+-ATPase and Kar2 in each step of secretory vesicle preparation was assayed by quantitative dot-blotting using specific monoclonal or polyclonal antibodies and ^{125}I-protein A (see Section 2).

[b]Integrated optical density units.

and Ca^{2+}-ATPase expression was induced by a temperature shift to 37°C for 2 h. Secretory vesicles were then isolated and assayed for Ca^{2+}-ATPase by quantitative dot-blotting. As summarized in Table 2, only 9% of the wild-type SR Ca^{2+}-ATPase present in the clarified lysate was recovered in the secretory vesicles. This value is very similar to the 8% recovery of the ER marker BiP/Kar2 and substantially lower than the 56% recovery of plasma membrane H^+-ATPase. Thus, it is likely that the trace amounts of SR Ca^{2+}-ATPase in the secretory vesicle fraction represent contamination with fragments of ER, and that little if any ATPase is able to exit the ER under the conditions of these experiments. As with wild-type Ca^{2+}-ATPase, *sec*-deficient cells expressing either H^+/Ca^{2+}-ATPase or 6×His-Ca^{2+}-ATPase were used to evaluate the ability of chimeric Ca^{2+}-ATPase to exit the ER (Table 2). There was a two-fold increase in the recovery of H^+/Ca^{2+}-ATPase and 6×His-Ca^{2+}-ATPase in the secretory vesicles fraction (18% and 20%) as compared with the wild-type control (9%) (Table 2). It is worth mentioning that the clarified lysate supernatant prepared according to the standard procedure for isolation of secretory vesicles [21] contained only a small fraction of the Ca^{2+}-ATPase present in the total lysate for both wild-type and chimeric Ca^{2+}-ATPase constructs (see Total lysate and Clarified lysate in Table 2). This indicates that most of the expressed SR Ca^{2+}-ATPase was discarded within the heavy fraction that sedimented at 14 500×*g* when preparing the clarified lysate (Table 2). Thus, the overall recovery of either wild-type or chimeric SR Ca^{2+}-ATPase in the secretory vesicle fractions was quite small, corresponding to approximately 0.5–1.1% of the total Ca^{2+}-ATPase initially present in the crude lysates (see Total lysate and Secretory vesicles in Table 2).

3.4. Phosphoenzyme formation and turnover of wild-type and chimeric Ca^{2+}-ATPase

To determine whether the chimeric Ca^{2+}-ATPase expressed in yeast was functional, enriched membranes recovered within the 24 000×*g* pellet were assayed for the ability to form the characteristic β-aspartyl phosphate intermediate upon incubation with [^{32}P]ATP. For this purpose, the method of Skerjanc et al. [5] was used, in which Ca^{2+}-ATPase is first immunoprecipitated, then phosphorylated and separated by acid gel electrophoresis. In the present work, chimeric Ca^{2+}-ATPase was solubilized from enriched yeast membrane fractions with the non-ionic detergent $C_{12}E_8$ and immunoprecipitated with anti-Ca^{2+}-ATPase monoclonal antibody and protein A-Sepharose. Wild-type Ca^{2+}-ATPase was used as a control in parallel (Fig. 4A). The immune complex was able to form a phosphoenzyme intermediate upon incubation with [γ-^{32}P]ATP in the presence of micromolar amounts of Ca^{2+} (Fig. 4A, lane EP). No band was seen in samples from control cells transformed with an empty plasmid vector (Fig. 4A, lane N). When the phosphorylated SR Ca^{2+}-ATPase was

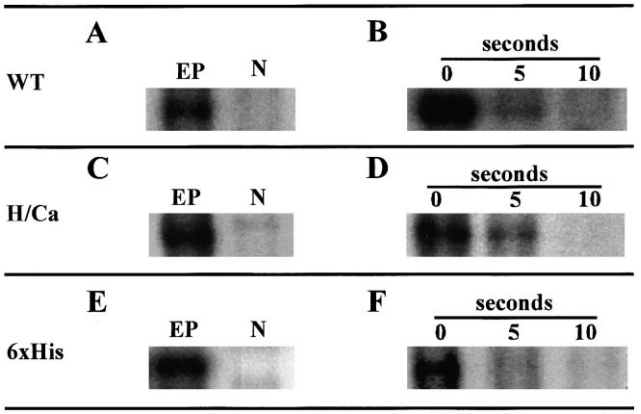

Fig. 4. Phosphorylation and phosphoenzyme decay of wild-type and N-terminal-tagged SR Ca^{2+}-ATPase. Yeast membrane fractions enriched in recombinant SR Ca^{2+}-ATPase were prepared from cells expressing either wild-type Ca^{2+}-ATPase (A and B), hexahistidine-tagged Ca^{2+}-ATPase (C and D) or H^+/Ca^{2+} chimeric ATPase (E and F) as described in Section 2. Aliquots containing 1 mg of total protein were collected and Ca^{2+}-ATPase was solubilized and immunoprecipitated as described in Section 2. Maximal levels of phosphoenzyme intermediate (EP) were measured (A, C and E) by reacting the immunoprecipitated ATPase on ice for 10 s in a medium containing 50 mM MOPS, pH 6.5, 80 mM KCl, 10 mM $MgCl_2$, 0.1 mM $CaCl_2$, 1 mg/ml $C_{12}E_8$, 0.5 mg/ml asolectin, 30% glycerol, 10 μM ATP and 40 μCi [γ-^{32}P]ATP. Reactions were stopped by addition of 10% TCA. Phosphoenzyme intermediate was detected after separation of samples on a 6% acrylamide acidic gel and exposure to an X-ray film. Yeast cells transformed with an empty plasmid were used as a negative control (N). Decay of phosphoenzyme (B, D and F) was measured by reacting the ATPase with radioactive ATP for 10 s as described above, followed by addition of 250 mM of non-radioactive ATP. Phosphorylation reaction was stopped by addition of 10% TCA after incubation with non-radioactive ATP for either 0, 5 or 10 s as indicated in the figure.

chased with excess cold ATP, the phosphoenzyme diminished in 5 s and had virtually disappeared by 10 s (Fig. 4B), indicating that it is capable of rapid turnover. Likewise, the ability of chimeric Ca^{2+}-ATPase to form a phosphorylated intermediate was tested by reacting detergent-solubilized and immunoprecipitated samples with [γ-^{32}P]ATP. An acid-stable phosphoenzyme intermediate was detected for both H^+/Ca^{2+}-ATPase and 6×His-Ca^{2+}-ATPase after acid gel electrophoresis and autoradiography (Fig. 4C,E, lane EP). The rate of decay of the phosphoenzyme intermediate was similar to that of wild-type ATPase, and no radioactive band was detected after a 10 s chase with non-radioactive ATP (Fig. 4D,F).

4. Discussion

In this work, we demonstrate that the bulk of wild-type SR Ca^{2+}-ATPase expressed in yeast under control of a heat shock promoter accumulates in a heavy fraction of ER membranes. The addition of the N-terminal portion of H^+-ATPase to the N-terminal end of SR Ca^{2+}-ATPase improved the ability of chimeric H^+/Ca^{2+}-ATPase to move along the secretory pathway, allowing it to accumulate in a light ER membrane fraction (Fig. 2) which has been associated in the literature with the smooth ER [31]. Interestingly, Degand et al. [7] observed in a recent work that the wild-type SR Ca^{2+}-ATPase expressed under control of the constitutive yeast PMA1 promoter accumulated in a light fraction of yeast ER. It is possible that the location of wild-type SR Ca^{2+}-ATPase in distinct ER subcompartments in each work is related to the different promoters employed.

When *sec*-deficient cells were transformed with either the H^+/Ca^{2+}-ATPase or the hexahistidine-tagged Ca^{2+}-ATPase cDNA, a two-fold increase in the amount of chimeric ATPase was found in secretory vesicles, as compared to wild-type enzyme. The increase can be accounted for by the presence of contaminant ER in the secretory vesicles fraction, as seen by detection of Kar2 ER marker in this fraction (Table 2).

A distinct shift was observed in the localization of chimeric ATPase, which accumulated predominantly in light ER, as opposed to wild-type ATPase that accumulated in heavy ER fractions. Since this effect was seen for both H^+/Ca^{2+}-ATPase or the hexahistidine-tagged Ca^{2+}-ATPase chimeras, a general effect of partial disruption of ER retention determinants, rather than one exerted by a particular targeting sequence present in the H^+-ATPase N-terminal portion (such as the conserved motif DDDIDALIEEL [10,32]), is probably responsible for the increased progression of the chimeric Ca^{2+}-ATPases along yeast ER. Conceivably, the addition of either H^+-ATPase or hexahistidine tags partially disrupts the ER retention signals present in native SR Ca^{2+}-ATPase. In this case, the chimeric Ca^{2+}-ATPases would accumulate in additional subcompartments of yeast ER, which may explain the remarkable three-fold increase in the overall expression level of both chimeras when compared with wild-type Ca^{2+}-ATPase. On the other hand, further progression along the secretory pathway is limited by the presence of additional ER retention signals located elsewhere in the Ca^{2+}-ATPase polypeptide, most likely within its first two transmembrane segments [33]. Recently, Boxembaum et al. [34] have obtained strong evidence indicating that the N-terminal region interacts with the first cytoplasmic loop, and eventually with the large cytoplasmic loop, to modulate the equilibrium kinetics of the Na^+,K^+-ATPase. The existence of analogous interactions in the SR Ca^{2+}-ATPase could provide the structural basis to explain the lack of ATPase activity in a truncated Ca^{2+}-ATPase chimera in which this domain was deleted [35].

We found that the corresponding region of yeast plasma membrane H^+-ATPase could not replace the N-terminal cytoplasmic moiety of SR Ca^{2+}-ATPase. The lack of expression of the deleted chimera points to the absence of functional conservation between the N-terminal domains of these two P-type cation-transporting ATPases. Previous findings from Skerjanc et al. [35] demonstrated that the removal of 32 N-terminal residues produced a non-functional ATPase but did not affect Ca^{2+}-ATPase expression and assembly in COS-1 cells. It is probable that the removal of 24 N-terminal residues from the Ca^{2+}-ATPase and its replacement with 88 N-terminal residues of yeast H^+-ATPase, as done in the chimeric $H^+\Delta Ca^{2+}$-ATPase construct, resulted in a misfolded enzyme and prevented the stable expression in yeast.

The quantitative recovery of wild-type and chimeric Ca^{2+}-ATPase in yeast membrane fractions follow-

ing medium- and high-speed centrifugations indicated that most of the recombinant Ca^{2+}-ATPase was inserted into the membrane. Moreover, both wild-type and chimeric Ca^{2+}-ATPases were functional as demonstrated by their ability to form a phosphorylated intermediate in the presence of ATP and Ca^{2+} and to undergo fast turnover. This evidence reinforces the assumption that targeting of the recombinant constructs was not limited by inadequate folding of the chimeric Ca^{2+}-ATPases. It should be noted that a fraction containing 25–30% of the chimeric Ca^{2+}-ATPase was not recovered by high-speed centrifugation and represents a portion of the expressed Ca^{2+}-ATPase that is not fully integrated in yeast membranes.

The modification of the SR Ca^{2+}-ATPase by addition of amino-terminal tags described in this work led to a three-fold increase in the amount of recombinant protein produced in yeast and a seven-fold increase in the enrichment of SR Ca^{2+}-ATPase in ER fractions, where it amounted to 7% of the total protein. This is similar to results reported for COS-1 microsomes, where expressed SR Ca^{2+}-ATPase typically represents 5% of membrane protein [3]. Thus, this approach may be useful to increase the yield of P-type ATPases [36,37] or other heterologously expressed integral membrane proteins [38] that are largely retained in the yeast ER. Additionally, the expression of functional N-terminal-tagged SR Ca^{2+}-ATPase constructs, such as the $6\times$His-Ca^{2+}-ATPase, paves the way for the development of a SR Ca^{2+}-ATPase purification scheme based on metal-chelating affinity chromatography [39–41].

Acknowledgements

We thank Dr. David H. MacLennan, University of Toronto, for supplying the Ca^{2+}-ATPase SERCA1 cDNA and the A52 monoclonal antibody, Dr. Mark D. Rose, Princeton University, for supplying the anti-BiP/Kar2 polyclonal antibody, Dr. Radovan Borojevic and Flavio Braga, Universidade Federal do Rio de Janeiro, for producing monoclonal antibody Cl-30 and Dr. Renato A. Mortara and Roberto Tedesco, Escola Paulista de Medicina, UNIFESP, for use of confocal microscopy facilities and technical expertise. This work was supported by grants from FAPESP and CNPq (to S.V.A) and NIH-FIRCA (to C.W.S. and S.V.A.).

References

[1] D.H. MacLennan, Biophys. J. 58 (1990) 1355–1365.
[2] D.H. MacLennan, W.J. Rice, N.M.J. Green, J. Biol. Chem. 272 (1997) 28815–28818.
[3] K. Maruyama, D.H. MacLennan, Proc. Natl. Acad. Sci. USA 85 (1988) 3314–3318.
[4] D.M. Clarke, T.W. Loo, G. Inesi, D.H. MacLennan, Nature 339 (1989) 476–478.
[5] I.S. Skerjanc, T. Toyofuku, C. Richardson, D.H. MacLennan, J. Biol. Chem. 268 (1993) 15944–15950.
[6] F. Centeno, S. Deschamps, A.M. Lompr, M. Anger, M.J. Moutin, Y. Dupont, P. Gjedde, J.M. Villalba, J.V. Moller, P. Falson, M. le Maire, FEBS Lett. 354 (1994) 117–122.
[7] I. Degand, P. Catty, E. Talla, D. Thines-Sempoux, A.D. d'Exaerde, A. Goffeau, M. Ghislain, Mol. Microbiol. 31 (1999) 545–556.
[8] E.M.R. Reis, C.W. Slayman, S. Verjovski-Almeida, Biosci. Rep. 16 (1996) 107–113.
[9] E.M.R. Reis, P.J.C. Biselli, S. Verjovski-Almeida, Annals of the Annual Meeting of the Sociedade Brasileira de Bioquímica e Biologia Molecular, 1996, p. 121 (Abstract).
[10] F. Portillo, I.F. de Larrinoa, R. Serrano, FEBS Lett. 247 (1989) 381–385.
[11] R. Elble, BioTechniques 13 (1992) 18–20.
[12] D.H. MacLennan, C.J. Brandl, B. Korczac, N.M. Green, Nature 316 (1985) 696–700.
[13] J. Sambrook, E.F. Fritsch, T. Maniatis, Molecular Cloning: A Laboratory Manual, Cold Spring Harbor Laboratory Press, Cold Spring Harbor, NY, 1989.
[14] M. Kozak, Proc. Natl. Acad. Sci. USA 87 (1990) 8301–8305.
[15] R. Gietz, A. Sugino, Gene 74 (1988) 527–534.
[16] R.K. Nakamoto, R. Rao, C.W. Slayman, J. Biol. Chem. 266 (1991) 7940–7949.
[17] E. Capieaux, M.-L. Vignais, A. Sentenac, A. Goffeau, J. Biol. Chem. 264 (1989) 7437–7446.
[18] R. Serrano, M.C. Kielland-Brandt, G.R. Fink, Nature 319 (1986) 689–693.
[19] D.S. Perlin, S.L. Harris, D. Seto-Young, J.E. Haber, J. Biol. Chem. 264 (1989) 21857–21864.
[20] A. Antebi, G.R. Fink, Mol. Biol. Cell 3 (1992) 633–654.
[21] A. Ambesi, K.E. Allen, C.W. Slayman, Anal. Biochem. 251 (1997) 127–129.
[22] O.H. Lowry, N.J. Rosebrough, A.L. Farr, R.J. Randall, J. Biol. Chem. 193 (1951) 265–275.
[23] C. Abeijon, P. Orlean, P.W. Robbins, C.B. Hirschberg, Proc. Natl. Acad. Sci. USA 86 (1989) 6935–6939.
[24] R.I. Feldman, M. Bernstein, R. Schekman, J. Biol. Chem. 262 (1987) 9332–9339.
[25] E. Harlow, D. Lane, Antibodies: A Laboratory Manual,

Cold Spring Harbor Laboratory Press, Cold Spring Harbor, NY, 1988.
[26] M.D. Rose, L.M. Misra, J.P. Vogel, Cell 57 (1989) 1211–1221.
[27] K.M. Hager, S.M. Mandala, J.W. Davenport, D.W. Speicher, E.J. Benz Jr., C.W. Slayman, Proc. Natl. Acad. Sci. USA 83 (1986) 7693–7697.
[28] J.R. Pringle, A.E.M. Adams, D.G. Drubin, B.K. Haarer, Methods Enzymol. 194 (1991) 565–602.
[29] C.M. Sanderson, J.S. Crowe, D.I. Meyer, J. Cell Biol. 111 (1990) 2861–2870.
[30] N.C. Walworth, P.J. Novick, J. Cell. Biol. 105 (1987) 163–174.
[31] C.M. Sanderson, D.I. Meyer, J. Biol. Chem. 266 (1991) 13423–13430.
[32] R. Serrano, Annu. Rev. Plant Physiol. Plant Mol. Biol. 40 (1989) 61–94.
[33] D. Foletti, D. Guerini, E. Carafoli, FASEB J. 9 (1995) 670–680.
[34] N. Boxenbaum, S.E. Daly, Z.Z. Javaid, L.K. Lane, R. Blostein, J. Biol. Chem. 273 (1998) 23086–23092.
[35] I.S. Skerjanc, D.M. Clarke, T.W. Loo, D.H. MacLennan, FEBS Lett. 336 (1993) 168–170.
[36] J.M. Villalba, M.G. Palmgren, G.E. Berberián, C. Ferguson, R. Serrano, J. Biol. Chem. 267 (1992) 12341–12349.
[37] A. Kerchove d'Exaerde, P. Supply, J. Dufour, P. Bogaerts, D. Thinès, A. Goffeau, M. Boutry, J. Biol. Chem. 270 (1995) 23828–23837.
[38] K. Kuchler, J. Thorner, Proc. Natl. Acad. Sci. USA 89 (1992) 2302–2306.
[39] J. Crowe, H. Dobeli, R. Gentz, E. Hochuli, D. Stuber, K. Henco, Methods Mol. Biol. 31 (1994) 371–387.
[40] F.C. Lanfermeijer, K. Venema, M.G. Palmgren, Protein Express. Purif. 12 (1998) 29–37.
[41] I. Sekler, R. Kopito, J.R. Casey, J. Biol. Chem. 270 (1995) 21028–21034.